Dalton Transactions

ROYAL SOCIETY OF CHEMISTRY

PAPER

View Article Online
View Journal | View Issue

Cite this: *Dalton Trans.*, 2021, **50**, 7474

Acetate intercalated Mg–Al layered double hydroxides (LDHs) through modified amide hydrolysis: a new route to synthesize novel mixed metal oxides (MMOs) for CO_2 capture†

G. V. Manohara, David Norris, M. Mercedes Maroto-Valer and Susana Garcia*

Layered double hydroxide (LDH) based mixed metal oxides (MMOs) are promising high temperature CO_2 capture sorbents. In order to improve their CO_2 capture capacity, it is crucial to bring in changes to their physicochemical properties such as morphology, particle size, surface area and activity by tuning the synthesis method. Here we report a modified amide hydrolysis method to synthesize LDHs with a mixed morphology and better CO_2 capture properties. Acetate intercalated Mg–Al LDHs with two different Mg/Al ratios (3 and 4) were synthesized by employing metal hydroxides as the starting precursors and acetamide as the hydrolysing agent. The resultant LDHs crystallized in a new morphology having a combination of both fibrous and sheet like crystallites. The MMOs derived from Mg–Al-acetate LDHs retained the mixed morphology observed in the precursor LDHs. The resultant MMOs showed almost a threefold increase in the BET surface area, 316 (Mg/Al = 3) and 341 (Mg/Al = 4) $m^2\ g^{-1}$, compared to MMOs derived from anion exchanged Mg–Al-acetate LDH (118 $m^2\ g^{-1}$). The MMOs synthesized by acetamide hydrolysis captured 1.2 mmol g^{-1} and 0. 87 mmol g^{-1} of CO_2 at 200 and 300 °C (atmospheric pressure), respectively. The CO_2 capture capacity realized was increased more than twofold compared to the CO_2 capture capacity of MMOs derived from anion exchanged acetate LDH (0.57 mmol g^{-1}) tested under similar conditions. The developed MMOs showed promising CO_2 capture (1.0 mmol g^{-1}) capacity at industrially relevant CO_2 concentration (14%).

Received 22nd February 2021,
Accepted 11th April 2021

DOI: 10.1039/d1dt00602a

rsc.li/dalton

1. Introduction

Anthropogenic CO_2 emissions are one of the major contributors to the greenhouse gas effect and are responsible for the rise in atmospheric temperature.[1] Carbon capture, usage and storage (CCUS) is one of the required pathways to minimize future emissions and to capture already emitted CO_2.[2,3] Adsorption by solid sorbents and absorption by liquid amines are two promising routes to capture anthropogenic CO_2.[4,5] Absorption by liquid amines is a well-known technology and it has been successfully tested on an industrial scale.[6,7] The health and environmental concerns and higher energy penalties limit the widespread implementation of liquid amines to capture CO_2.[8] On the other hand, adsorption by solid sorbents is a promising alternative due to (a) ease of operation and handling, (b) wide window of operating temperature, (c) operation at both high and low CO_2 concentrations, (d) tunability of selectivity and activity, and (e) their low specific heat capacities.[9,10]

Among the solid sorbents, layered double hydroxides (LDHs) based mixed metal oxides (MMOs) stand apart due to their various physiochemical properties that make them ideal candidate materials for CO_2 capture.[11–14] LDHs are a class of layered solids having derived their structure from that of the mineral brucite, $Mg(OH)_2$.[15] LDHs are represented by the general formula $[M^{2+}_{1-x}M^{3+}_{x}(OH)_2]^{x+}(A^{-x/n})\cdot yH_2O$, where M^{2+} = Mg, Co, Ni, Ca, and Zn, M^{3+} = Al, Fe, and Ga, A = anion (organic or inorganic ions), $0.15 \geq x \leq 0.33$ and $0.5 \geq y \leq 1.0$.[16] LDHs and LDH derived MMOs have been used as catalysts, as precursors to catalysts, as electrodes in batteries and supercapacitors, as sensors, as fillers in nanocomposites, and as sorbents in various applications.[17,18] Among all the applications of LDHs and MMOs, medium-to-high temperature (200–650 °C) CO_2 capture is one widely studied topic.[19] LDH derived MMOs are ideal candidate materials for CO_2 capture due to (a) fast adsorption/desorption kinetics, (b) large untapped theoretical capture potential, (c) the ability to work under flue gas conditions, (d) ease of preparation and handling, and (e) economical and environmentally benign nature.[20,21]

Research Centre for Carbon Solutions (RCCS), School of Engineering and Physical Sciences, Heriot-Watt University, Edinburgh EH14 4AS, UK.
E-mail: s.garcia@hw.ac.uk

†Electronic supplementary information (ESI) available. See DOI: 10.1039/d1dt00602a

Despite all the promising properties of better CO_2 capture sorbent materials, MMOs are yet to live up to their potential due to their (a) low CO_2 capture capacity, (b) poor thermal and mechanical stability, and (c) capacity fading during cycling.[22] To overcome these limitations, various attempts to improve their CO_2 capture capacity have been reported in the literature.[23,24] For instance, LDHs are substituted with varied layered metal cations and interlayer anions; alkali metals and metal carbonates are doped with LDH based MMOs; to improve the mechanical and thermal stability of MMOs for better CO_2 capture and cycling performance, LDHs are supported with zeolites, carbon nanotubes (CNT), and graphite oxide (GO).[25–28] Likewise, different synthesis methods such as aqueous exfoliation and post synthesis washing with organic solvents are also employed to improve the surface area and CO_2 capture capacity of MMOs.[29,30]

Furthermore, the properties of MMOs such as basicity, particle size, porosity, and morphology can be tuned by altering the combination of pre- and post-synthesis conditions such as composition, synthesis method, starting precursors, time and rate of addition of reagents, supersaturation and drying/washing methods of precursor LDHs.[27–29] LDHs prepared by one synthesis method differ greatly from those prepared by other methods. As an example, LDHs prepared by co-precipitation show ill-defined hexagonal crystallites having submicron particle sizes, whereas LDHs prepared by hydrothermal methods employing the homogeneous precipitation from solution (HPFS) method show a crystalline hexagonal morphology with micron sized particles.[31,32] Similarly, samples prepared with the help of surfactants show distinct morphology and properties compared to those prepared without the use of surfactants.[33] In addition, different hydrolysing agents such as urea, formamide and acetamide having different hydrolysing constants result in LDHs with different anions, and hence different properties.[34,35]

An improved basicity of LDHs coupled with a varied morphology is expected to generate novel MMOs having better CO_2 capture properties. Generally, metal salts such as metal nitrates and chlorides are employed as the source of metal cations in the synthesis of LDHs. These precursor metal salts are highly acidic and could influence the basicity of the resultant LDHs. Unitary hydroxides such as $Mg(OH)_2$ and $Al(OH)_3$ are highly basic compared to metal salts such as metal nitrates or metal chlorides.[36,37] Employing these unitary hydroxides as the source of metal cations instead of metal salts in LDH synthesis could affect the overall basicity of the resultant LDHs and their derived MMOs. These unitary hydroxides were employed as the source of metal cations in the synthesis of LDHs with interesting properties.[38–40] The morphology of LDHs could be tuned by changing the hydrolysing agent and that will alter the surface properties of LDHs and their derived MMOs.[34,35] In this paper, we attempted to bring in a new and interesting morphology of LDHs by modifying the synthesis method and by changing the starting metal precursors.

Modified amide hydrolysis was employed to synthesize Mg–Al-acetate LDHs starting with metal hydroxides instead of metal salts. Acetamide was used as the hydrolysing agent to facilitate the nucleation of the metal cations by providing the necessary base (NH_4OH) and also acts as the source of anions (CH_3COO^-).[41] The MMOs derived from the as-synthesized LDHs were studied for CO_2 capture at different temperatures under both CO_2 rich (86%) and lean (14%) conditions.

2. Experimental

2.1. Synthesis

All the chemicals, $Mg(OH)_2$, $Al(OH)_3$, acetamide, $Mg(NO_3)_2{\cdot}6H_2O$, $Al(NO_3)_3{\cdot}9H_2O$, NaOH and sodium acetate were purchased from Sigma Aldrich and used as received. Deionised water (18 MΩ cm resistivity, millipore water purification system) was used throughout the experiments. LDHs with two different Mg/Al ratios (3 and 4) were synthesized (acetamide to metal ion ratio, acetamide/M = 5). In a typical experiment, the stoichiometric amounts of $Mg(OH)_2$, $Al(OH)_3$ and acetamide (acetamide/metal = 5) were taken in 100 mL of water. The reaction mixture was stirred at room temperature for an hour to obtain a homogeneous mixture. The resultant reaction mixture was transferred to a Teflon lined vessel and hydrothermally treated at 180 °C for 24 h. The resultant Mg–Al-acetate LDH was recovered by filtration followed by drying at 65 °C overnight. For comparison, Mg–Al-acetate (Mg/Al = 3) LDH was prepared by the anion exchange reaction (10 times excess acetate ion used) starting from Mg–Al–NO_3 LDH. In this case, the precursor Mg–Al–NO_3 LDH (Mg/Al = 3) was synthesized by employing the co-precipitation method (pH 9). The pH of the reaction mixture was maintained at 9 by the constant addition of 1 N NaOH solution (Metrohm auto titrator). The temperature of the reaction mixture was maintained at 70 °C while stirring. Next, 0.5 g of Mg–Al–NO_3 LDH was dispersed in 100 mL of hot deionised water (80 °C) and to this mixture, 10 times excess stoichiometric amount of acetate ion was added in the form of sodium acetate. The reaction mixture was stirred for 24 h at 70 °C using a magnetic stirrer. The resultant Mg–Al-acetate LDH was recovered by centrifugation and washed with a copious amount of water.

The commercial LDH Pural MG70 sample was procured from SASOL for benchmarking the performance of the obtained samples.

2.2. Characterization

Powder X-ray Diffraction (PXRD) patterns were recorded on a Bruker D8 Advance powder diffractometer, using Ge-monochromated Cu-Kα1 radiation (λ = 1.5406 Å) from a sealed tube, operating at 40 kV and 40 mA with a LynxEye linear detector in reflectance mode. Data were collected over the angular range of 5–70° 2θ with a step size of 0.009° over one hour span. The Fourier Transform Infrared spectra (FTIR) of samples were measured using a PerkinElmer spectrometer in ATR mode (4000 to 600 cm^{-1}). The elemental analysis of Mg^{2+} and Al^{3+} (ICP-OES) was carried out by the atomic emission technique using a PerkinElmer Optima 5300 DV. A mixture of concen-

trated nitric acid and hydrochloric acid in the ratio of 1 : 3 was used to dissolve the LDH. The solution was diluted 20 times prior to analysis. The C, H and N analysis of the LDH samples was carried out by taking approximately 3 mg of samples and placing them in a tin capsule, followed by combustion in a high oxygen environment at 950 °C using an Exeter Analytical CE-440 elemental analyser calibrated with acetanilide. Surface area analysis of the sample was carried out by the gas adsorption technique (N_2, 77 K) using a Micromeritics Gemini VII surface analyser. Prior to the gas adsorption measurement, the sample was degassed for 3 h at 150 °C. The surface morphology of the sample was characterized by scanning electron microscopy (SEM) using an FEI Quanta FEG SEM.

2.3. CO_2 capture studies

Thermal analysis and CO_2 capture studies were performed using a thermogravimetric analyser (TA Instruments TA 500). Pristine Mg–Al-acetate LDHs were used instead of preformed MMOs to avoid CO_2 contamination. Freshly prepared LDHs were loaded into a platinum pan and decomposed under an inert atmosphere (using 100 mL min^{-1} N_2, 4 h, 400 °C, 10 °C min^{-1}). Once the decomposition was completed, the temperature was brought back to the desired capture temperature and CO_2 gas was switched on (for 2 h) to test the uptake capacity of the resultant MMOs. The CO_2 capture capacity of the resultant MMOs was tested at two different CO_2 concentrations, 86 and 14% (mixed with N_2), and at three different temperatures (200, 250 and 300 °C). For comparison, the CO_2 capture capacity of MMOs generated from the commercial Pural MG70 LDH was measured at 200 °C under 86% CO_2 and under the same conditions as those used for Mg–Al-acetate LDHs. Next, the cyclic behaviours (10 cycles) of the Mg–Al-acetate (Mg/Al = 3 and 4) and commercial Pural MG70 LDH derived MMOs were investigated under 86% CO_2. Adsorption at 200 °C was carried out for 2 h and the regeneration was carried out using N_2 gas at 400 °C (2 h, 10 °C min^{-1}).

3. Results and discussion

3.1. Synthesis and characterization of acetate intercalated LDHs and MMOs derived from them

Hydrolysis of acetamide proceeds according to the equation given below:

$$CH_3CONH_2 + H_2O \rightarrow CH_3COOH + NH_3$$

Depending on the pH of the reaction medium, hydrolysis of acetamide could be either base or acid catalysed.[42] Synthesis of acetate intercalated LDHs by the conventional co-precipitation or anion exchange reactions requires large excess of acetate ions due to their high solubility in water (high hydration enthalpy).[43] On the other hand, acetamide hydrolysis is a better alternative to prepare acetate intercalated LDHs, as explained next. Acetamide hydrolysis generates carboxylic acid (acetic acid) and ammonia. The resultant acetic acid will serve as the source of acetate ions and ammonium will act as a base to precipitate the metal hydroxides.[41] This method is similar to the synthesis of LDHs by urea (amide) hydrolysis.[44] Acetamide hydrolysis was successfully used to prepare Ni–Al-acetate LDHs and attempts to prepare Mg–Al LDHs were largely unsuccessful.[41] The successful synthesis of metal hydroxides with varied metal cations largely depends on the pH of the reaction medium and this in turn depends on the starting metal ion precursors (metal nitrates, metal chlorides, metal oxides/metal hydroxides, *etc.*).[37,45] In the case of Al^{3+} containing LDHs, the synthesis mainly depends on the formation pH of divalent cations, as the Al^{3+} is amphoteric in nature and precipitates in both acidic and basic media. Specifically, LDHs of Ni^{2+} or Co_2^{+} with Al^{3+} form at pH 5–6, whereas Mg–Al LDHs form between pH 9 and 10.[37,45] The lower pH of the reaction medium (between 5 and 6) and metal nitrates as the starting precursors could be the possible reasons for not realizing Mg–Al-acetate LDHs in previous attempts.[41] In this paper, we have attempted to synthesize Mg–Al-acetate LDHs through acetamide hydrolysis by employing metal hydroxides [$Mg(OH)_2$ and $Al(OH)_3$] as the starting precursors for metal cations instead of metal nitrates/chlorides. The basic nature of metal hydroxides compared to largely acidic metal salts, is expected to increase the pH of the reaction medium and thus favour the successful synthesis of Mg–Al-acetate LDHs.

We prepared Mg–Al-acetate LDHs with two different Mg/Al ratios (3 and 4), as described in the Experimental section. The metal contents of the resultant compounds were determined by the ICP-OES method and the anion content was determined by CHN analysis. We derived the empirical formula of the resultant compounds by combining the results of the chemical analyses as follows; $[Mg_{0.72}\ Al_{0.28}\ (OH)_2]\ (CH_3COO)_{0.28}{\cdot}0.4\ H_2O$ (Mg/Al = 3) and $[Mg_{0.78}\ Al_{0.22}\ (OH)_2]\ (CH_3COO)_{0.22}{\cdot}0.5\ H_2O$ (Mg/Al = 4). The Mg/Al ratio of the resultant LDHs has slightly deviated from that of the initial reaction mixture used for the synthesis. This deviation in the Mg/Al ratio is widely seen in the literature and could be largely due to varied physical constants of the two different unitary metal hydroxides involved.[45]

The PXRD patterns of the Mg–Al-acetate LDHs synthesized by acetamide hydrolysis are shown in Fig. 1. Mg–Al-acetate LDH with Mg/Al = 3 shows (Fig. 1a) the first three basal reflections at 12.34 (7.15), 6.24 (14.16) and 4.16 Å (21.31° 2θ). These basal reflections match with the hydrated phase of acetate intercalated LDH reported in the literature.[41] A *d*-spacing of 12.34 Å also indicates that the bilayer arrangement of the acetate ion is perpendicular to the metal hydroxide layers in the interlayer space.[41,43] Similarly, Mg–Al-acetate LDH with Mg/Al = 4 shows (Fig. 1b) the basal reflections at 12.30 (7.18), 6.21 (14.24) and 4.13 Å (21.50° 2θ), which match with the hydrated phase of acetate intercalated LDH.[41] The crystalline nature of both samples is evident from the sharp basal reflections observed in their PXRD patterns. In addition to the basal reflections, the appearance of turbostratically disordered mid 2θ region (around 35° 2θ) and weak 2D reflections (around 60–62° 2θ) which are characteristics of LDHs confirm the formation of Mg–Al-acetate LDHs *via* acetamide hydrolysis.[41] The

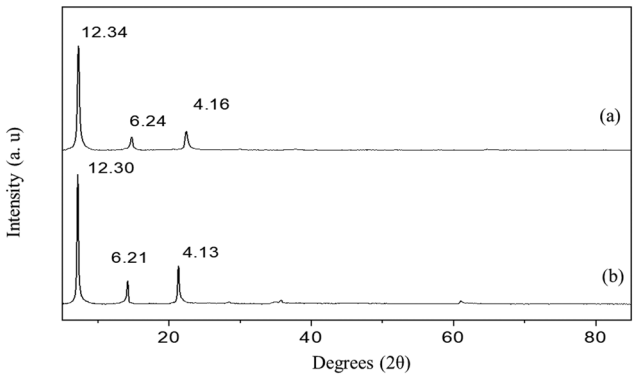

Fig. 1 PXRD patterns of Mg–Al-acetate LDHs prepared by acetamide hydrolysis (a) Mg/Al = 3 and (b) Mg/Al = 4. The values correspond to the *d*-spacing in Å.

successful synthesis and the intercalation of the acetate ion was further characterized by Fourier transform infrared spectroscopy (FTIR). Mg–Al-acetate LDH with Mg/Al = 3 shows two strong vibrations at 1410 and 1557 cm^{-1} and they could be assigned to symmetric and antisymmetric stretching vibrations of the carboxylic group COO^-, respectively (Fig. 2a).[46] It also shows a broad vibration centered at 3350 cm^{-1}, and this could be assigned to hydrogen bonded hydroxyl ions and intercalated water molecules.[46] The shoulder observed at 1340 cm^{-1} corresponds to the bending mode of the $-CH_3$ group of the acetate ion. The metal–metal (M–M) and metal–oxygen (M–O) vibrations which are present below 1000 cm^{-1} are not clearly resolved. Similarly, Mg/Al = 4 also shows (Fig. 2b) vibrations at 1340, 1410, 1558 and 3350 cm^{-1} corresponding to carboxylate and hydroxyl ions, as described above. The FTIR spectra of both samples (Mg/Al = 3 and 4) corroborate the presence of an intercalated acetate ion and also confirms the successful formation of Mg–Al-acetate LDHs. Besides carboxylate (COO^-) and hydrogen bonded hydroxyl ions (OH^-) no other vibration are seen in the FTIR spectra, which clearly indicates the absence of any impurities including the starting metal hydroxide precursors. The thermal behaviour of the resultant samples was studied using TGA and the results are presented

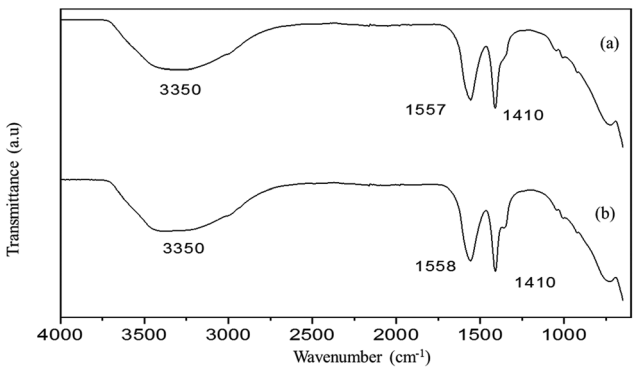

Fig. 2 FTIR spectra of Mg–Al-acetate LDHs prepared by acetamide hydrolysis (a) Mg/Al = 3 and (b) Mg/Al = 4.

in Fig. S1.† Both samples show a mass loss behaviour typical of acetate intercalated LDHs as reported in the literature.[41] The mass loss observed below 200 °C can be assigned to the elimination of adsorbed and intercalated water. Dehydroxylation and the elimination of intercalated acetate ions were observed between 200 and 400 °C. The surface morphology of the resultant Mg–Al-acetate LDHs (Fig. 3) was characterized by SEM. Both samples showed an unusual mixed morphology having sheet-like and fibrous-like crystallites. LDHs generally exhibit a hexagonal sheet-like or sand rose morphology.[47] The observed morphology having fibrous-like crystallites along with sheet-like ones is somewhat unusual and could be due to the presence of secondary phases.

To verify the presence of secondary phases as impurities, we compared the PXRD patterns of the resultant LDHs with those of the starting precursors, *i.e.* $Mg(OH)_2$, $Al(OH)_3$, and acetamide (Fig. S2†). The PXRD patterns of the resultant LDHs do not show peaks that correspond to any of the starting precursors. Similarly, the FTIR spectra of the starting precursors do not match with those of the resultant LDHs (Fig. S3†), indicating the absence of any of these as secondary phases in the resultant LDHs. However, it has been previously reported that compounds prepared by acetamide hydrolysis show fibrous morphology.[48,49] The concentration of acetamide in the reaction mixture, the time and the temperature are known to have significant effects on the morphology of the resultant compounds.[48,49] Thus, the observed mixed morphology along with fibrous crystallites corroborates the previous finding for samples prepared by acetamide hydrolysis.[48,49] The Ni–Al-acetate LDHs prepared by acetamide hydrolysis using metal nitrates showed a sand rose morphology.[41] The observed mixed morphology in the present case could be due to the combined effect of the starting precursors and the concentration of the acetamide.

In order to investigate the effect of the synthesis method and different starting precursors on the CO_2 capture properties of the resultant LDH derived MMOs, Mg–Al-acetate LDH (Mg/Al = 3) was prepared by the anion exchange reaction starting from the Mg–Al–NO_3 precursor. The PXRD pattern of anion exchanged Mg–Al–acetate LDH shows (Fig. S4†) basal reflections at 12.56 (7.03), 6.33 (13.97) and 4.20 Å (21.14° 2θ). This phase corresponds to hydrated acetate intercalated LDHs.[43] Anion exchanged acetate LDH also shows 2*d* reflection around 1.50 Å (61.60° 2θ), which corresponds to the *ab* plane of the hydroxide sheet. The PXRD pattern also shows the turbostratically disordered reflection at 2.60 Å (34.58° 2θ), typical of hydrated acetate intercalated LDH.[43] The intercalation of acetate was further characterized by FTIR spectra, as shown in Fig. S5.† The sample shows stretching vibrations due to the carboxylate ion (1553 and 1410 cm^{-1}) and the hydrogen bonded hydroxyl ion (3312 cm^{-1}), confirming the formation of Mg–Al-acetate LDH.[43] The surface of the anion exchanged acetate LDH was characterized by SEM and it shows the surface morphology typical of the LDHs (Fig. S6a† and 6b). Interestingly, the mixed morphology having fibrous crystallites observed in the LDHs prepared by acetamide hydrolysis is absent in the anion exchanged acetate LDH.

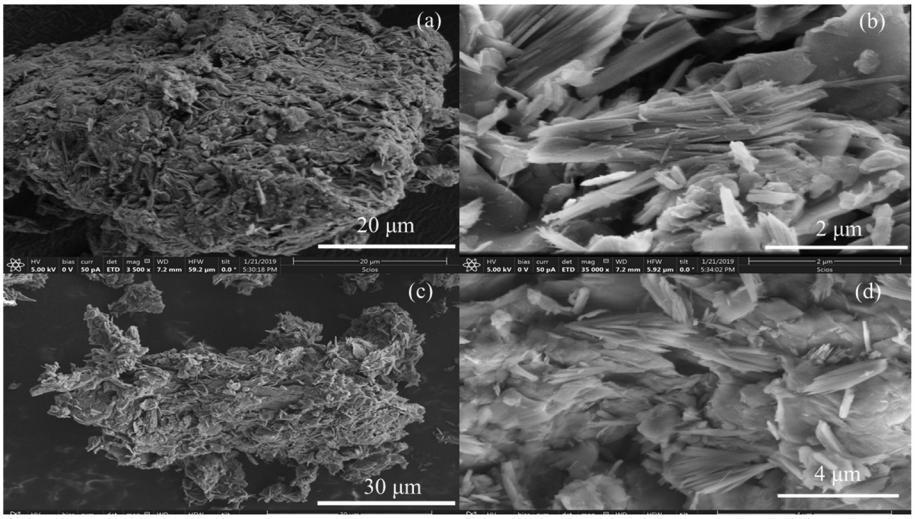

Fig. 3 SEM images of Mg–Al-acetate LDHs prepared by acetamide hydrolysis (a and b) Mg/Al = 3 and (c and d) Mg/Al = 4.

The targeted LDH derived MMOs for CO_2 capture studies were obtained by decomposing Mg–Al-acetate (Mg/Al = 3 and 4) LDHs at 400 °C for 4 h under a N_2 atmosphere. The PXRD patterns of the resultant MMOs are shown in Fig. 4. Thermal decomposition of Mg–Al LDHs at or around 400 °C results in the formation of MMOs, and understanding the exact chemical and structural properties of these materials is an ongoing research.[50–52] The only crystalline phase observed in the resultant MMOs is MgO and the nature of the aluminium containing oxide/hydroxide is amorphous. MMOs derived from Mg–Al-acetate LDHs show (Fig. 4a and b) reflections at 2.10 (43.02° 2θ) and 1.48 Å (62.51° 2θ), which correspond to MgO of the MMOs phase.[53] The absence of reflections other than the ones corresponding to MgO in the resultant MMOs again confirms the absence of any crystalline impurities/secondary phases in the parent LDHs as well as in the derived MMOs.

The surface morphology of the resultant MMOs was studied using SEM. The SEM images of the MMOs are presented in Fig. 5, and MMOs from both LDHs (Mg/Al = 3 and 4) show a similar morphology to the one observed in the parent Mg–Al-acetate LDHs (Fig. 3). MMOs have retained the mixed morphology even after thermal decomposition, which indicates the topotactic conversion of precursor LDHs to the resultant MMOs.[54] The mixed morphology involving fibrous crystallites could influence the properties of the resultant MMOs, which in turn could show different CO_2 capture performances.

The anion exchanged acetate LDH was also decomposed to obtain MMOs, as described in the Experimental section. The PXRD pattern of MMOs derived from anion exchanged LDH is shown in Fig. S7† and it shows peaks due to MgO at 2.08 (43.36) and 1.47 Å (62.92° 2θ) as expected.[53] The morphologies of the resultant MMOs are given in Fig. S6c† and 6d and they are similar to the ones reported in the literature for LDH derived MMOs.[55]

The surface area of the resultant MMOs was studied using the N_2 gas adsorption technique as discussed in the Experimental section. All the samples show the type IV adsorption isotherm characteristic of mesoporous solids (Fig. 6).[56] The samples show a H2 type hysteresis loop between 0.5 and 1.0 pressure range, which is associated with the ink bottle pores indicating the mesoporous nature of the MMOs. The surface area of the samples was calculated using the BET method, and the pore size and pore volume were calculated by the BJH method and using the desorption branch of the isotherm. The surface properties of all the MMOs are given in Table 1.

The MMOs generated by acetamide hydrolysis show very good surface area compared to the MMOs generated by the anion exchange method. The observed large surface areas of MMOs generated by acetamide hydrolysis are amongst the highest values reported so far for LDH based MMOs.[30] The synthesis method along with mixed morphology involving fibrous crystallites could be a major factor in creating that high surface area.

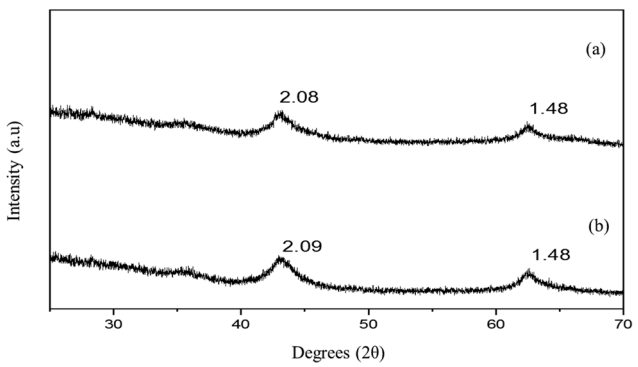

Fig. 4 PXRD patterns of MMOs derived from Mg–Al-acetate LDHs prepared by acetamide hydrolysis (a) Mg/Al = 3 and (b) Mg/Al = 4. The values correspond to the *d*-spacing in Å.

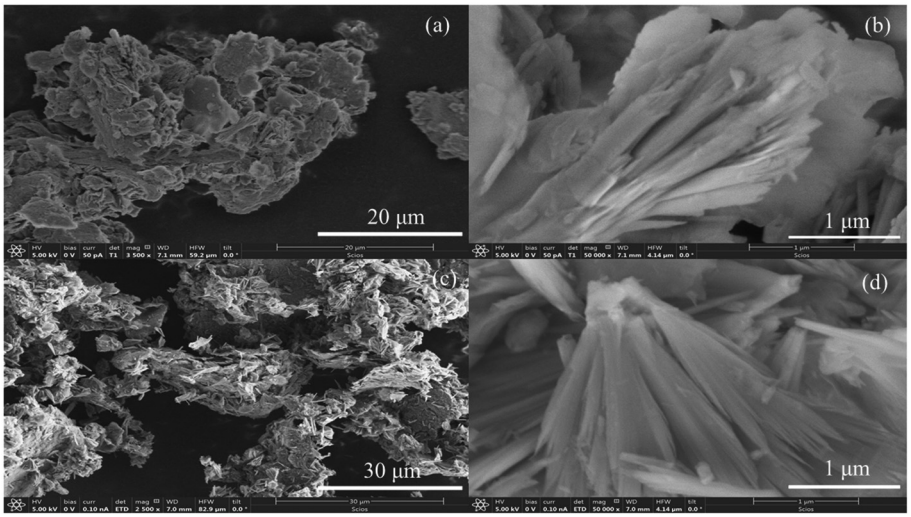

Fig. 5 SEM images of MMOs derived from Mg–Al-acetate LDHs prepared by acetamide hydrolysis (a and b) Mg/Al = 3 and (c and d) Mg/Al = 4.

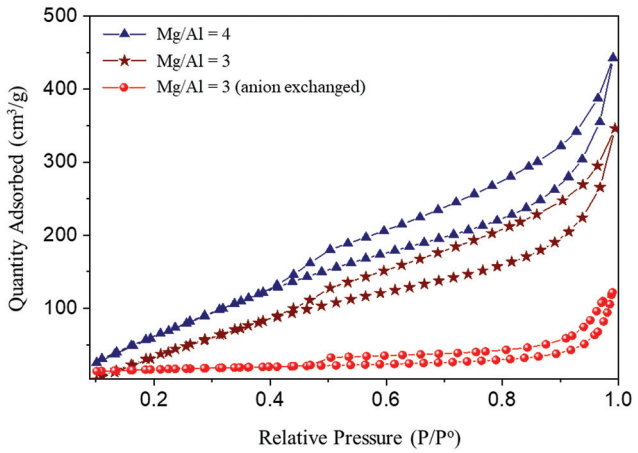

Fig. 6 N_2 adsorption isotherms (77 K) of MMOs derived from Mg–Al-acetate LDHs prepared by acetamide hydrolysis and the anion exchange method.

Table 1 Surface properties of MMOs generated by acetamide hydrolysis and the anion exchange method

Sample	Surface area ($m^2\ g^{-1}$)	Pore volume ($cm^3\ g^{-1}$)	Pore size (nm)
Anion exchanged (Mg/Al = 3)	118.6	0.25	11.91
Acetamide hydrolysis (Mg/Al = 3)	316.2	0.68	5.00
Acetamide hydrolysis (Mg/Al = 4)	341.7	0.75	4.84

3.2. CO_2 capture studies of MMOs derived from acetate intercalated LDHs

CO_2 capture studies on MgO and MMOs derived from Mg–Al LDHs are usually carried out at around 200–250 °C. The mechanism of CO_2 adsorption over MMOs is not yet clear, but it is broadly assumed that it is due to chemisorption.[57] The earlier studies of CO_2 capture on MMOs showed the evidence for metal carbonate formation during the CO_2 sorption over LDH derived MMOs.[58] The MgO present in the MMOs is found to be the active phase for the formation of metal carbonates. Assuming chemisorption as the adsorption mechanism, one would expect that the formation of metal carbonates would take place based on the amount of MgO present in the MMOs. However, the amount of CO_2 capture realized for LDH derived MMOs is very negligible (2–5%) when compared to the amount of MgO present.[22]

In this work, CO_2 capture studies of the resultant MMOs are carried out as described in the Experimental section. The CO_2 capture performance of the obtained MMOs was evaluated in the range from 200 to 300 °C at atmospheric pressure and under both CO_2 rich (86% CO_2) and more diluted (14% CO_2) conditions, and it is presented in Fig. 7.

MMOs derived from 4 : 1 LDH showed a CO_2 capture capacity (86% CO_2) of 1.19 mmol g^{-1} at 200 °C, which decreased to 0.87 mmol g^{-1} at 300 °C. This reduction in the capture capacity at 300 °C from that at 200 °C is similar to that previously reported in the literature.[30]

However, the CO_2 capture capacity observed at 200 °C is one of the highest values reported so far for pristine/unpromoted MMOs (Table 2).[20,59] The observed CO_2 capture capacity represents a very significant improvement compared to the capture capacity previously reported for acetate LDH derived MMOs (0.56 mmol g^{-1}).[60] Similarly, MMOs derived from 3 : 1 LDH showed better CO_2 capture capacities than the previously reported values, with capture capacities of 1.02 mmol g^{-1} (86% CO_2) at 200 °C and 0.7 mmol g^{-1} at 300 °C.[60] MMOs derived from 4 : 1 LDH showed better CO_2 capture capacities at all temperatures than those derived from 3 : 1 LDH. The higher uptake could be due to the higher amount of Mg^{2+} present in the MMOs derived from 4 : 1 LDH. For comparison, the CO_2 capture capacity of MMOs derived from the commercial LDH

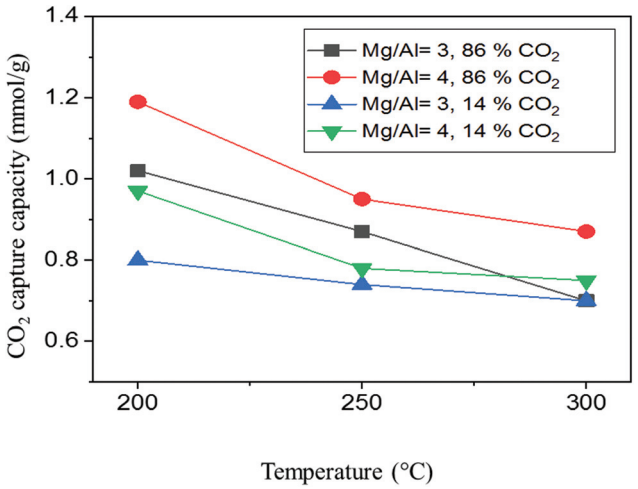

Fig. 7 CO_2 capture capacity (under 86 and 14%CO_2) of MMOs derived from Mg–Al-acetate LDHs synthesized by acetamide hydrolysis as a function of temperature.

Pural MG70 (Mg/Al = 2.33) was tested at 200 °C under 86% CO_2. The sample showed a CO_2 capture capacity of 0.67 mmol g^{-1} which is much lower than the capture capacity achieved for the MMOs derived from Mg–Al-acetate LDHs synthesized by acetamide hydrolysis. The CO_2 capture profiles of MMOs derived from both 3 : 1 and 4 : 1 LDHs were studied at 200, 250 and 300 °C and are given in Fig. S8.† All the samples showed a very rapid initial uptake of CO_2 followed by a slow and steady uptake. None of the samples reached equilibrium within 2 h of experimental time. However, the samples captured more than 80% of CO_2 within the first 10–15 min compared to the overall capture capacity achieved over 2 h (the inset of Fig. S8†).

The MMOs derived from Mg–Al-acetate LDHs were also tested under more industrially relevant flue gas CO_2 concentrations (14%). Under these conditions, MMOs derived from 4 : 1 LDH showed a CO_2 uptake of 0.97 mmol g^{-1} at 200 °C whereas MMOs derived from 3 : 1 LDH showed 0.80 mmol g^{-1}. The amount of CO_2 captured by both MMOs decreased as the temperature was increased from 200 to 300 °C. The observed CO_2 capture capacities of MMOs synthesized by acetamide hydrolysis were compared with the literature reported CO_2 values of pristine MMOs, as shown in Table 2. It can be seen that MMOs generated from the Mg–Al-acetate LDHs synthesized by modified acetamide hydrolysis show better CO_2 capture capacities than the previously reported ones.

The reduced CO_2 capture capacity of MMOs under 14% CO_2 compared to 86% CO_2 is as expected due to the lower partial pressure of CO_2. However, the CO_2 uptake under 14% CO_2 is higher than most of the values reported for MMOs even under 100% CO_2.[59–61] This significant increase in the CO_2 capture capacity could be due to the combination of different factors including the starting metal ion precursors, synthesis method, hydrolysing agent and observed morphology. Generally, metal salts (nitrates and chlorides) are employed as precursors to metal ions in the synthesis of LDHs, which are highly acidic. In the present case, highly basic metal hydroxides are used as metal ion precursors and this could have slightly altered the basicity of the resultant LDHs. This change in the starting precursors could have also altered the local pH and this in turn could have a significant effect on the nucleation and growth of the LDH. This is evident from the unsuccessful previous attempts to prepare Mg–Al-acetate LDHs starting with metal nitrates using acetamide hydrolysis.[41]

The surface properties of MMOs depend on the morphology and any change in that morphology will alter their properties. The combination of the starting precursors with the hydrolysing agent and synthesis method has resulted in a new mixed morphology involving fibrous and sheet-like crystallites of the resultant Mg–Al-acetate LDHs.

To evaluate the effects of the synthesis method and starting precursors on the CO_2 capture performance of the materials, we also tested the CO_2 capture capacity of MMOs derived from

Table 2 Comparison of CO_2 capture capacities of Mg/Al LDH based MMOs reported in the literature with the MMOs generated by the acetamide hydrolysis method

Precursor LDH sample	CO_2 capture temperature (°C)	CO_2 concentration (%)	CO_2 capture capacity (mmol g^{-1})	Ref.
Mg–Al–CO_3	200	100	0.8	62
Mg–Al–CO_3	200	50	0.9	63
Mg–Al–Pl	200	100	0.91	64
Mg–Al–CO_3	240	100	0.83	65
Mg–Al–St	200	100	1.15	66
Mg–Al–St	300	100	1.01	67
Mg–Al–CO_3	200	100	0.74	68
Mg–Al–Ac	200	100	0.51	64
Mg–Al–CO_3	300	100	0.62	69
SASOL MG70	200	86	0.67	This work
Mg–Al–Ac	200	86	1.20	This work
Mg–Al–Ac	200	86	1.02	This work
Mg–Al–Ac	200	14	0.97	This work
Mg–Al–Ac	200	14	0.80	This work

CO_3 = carbonate, Pl = palmitate, St = stearate, and Ac = acetate. The CO_2 capture capacities reported in Table 2 were measured using the TGA technique.

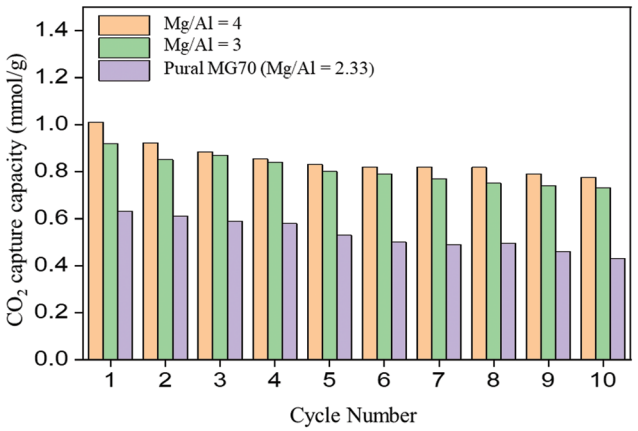

Fig. 8 CO_2 capture cycling study (under 86% CO_2) of MMOs derived from Mg–Al-acetate LDHs synthesized by acetamide hydrolysis and Pural MG70 LDH. The carbonation was carried out at 200 °C and the regeneration was carried out at 400 °C.

anion exchanged Mg–Al-acetate LDH. They showed a CO_2 capture of 0.57 mmol g^{-1} at 200 °C under 86% CO_2. This observed CO_2 capture capacity is similar to the reported value (0.56 mmol g^{-1}) for acetate LDH derived MMOs under similar testing conditions.[54] This clearly highlights the need for alternative strategies in developing improved LDH based MMOs for medium-to-high temperature CO_2 capture applications. The MMOs derived from Mg–Al-acetate LDHs synthesized by acetamide hydrolysis were tested for cyclic CO_2 stability and the results were compared with the CO_2 cyclic stability of MMOs derived from the commercial LDH Pural MG70. The results are presented in Fig. 8. The MMOs derived from Mg–Al-acetate LDH (Mg/Al = 4) retained 65% (0.77 mmol g^{-1} CO_2) of their initial capture capacity after 10 adsorption/regeneration cycles. On the other hand, MMOs generated from Mg–Al-acetate LDH (Mg/Al = 3) showed a better stability as the capture capacity loss was around 28% after 10 cycles. This improved CO_2 cycling stability might be attributed to the additional aluminium present in the sample compared to the MMOs having Mg/Al = 4 (lower aluminium content).[20,70] The commercial LDH based MMO sorbents (Pural MG70) showed a 35% loss in the capture capacity after 10 cycles. The CO_2 capture capacity retained by the commercial LDH based MMOs after 10 cycles (0.43 mmol g^{-1}) was much less than the MMOs derived from the Mg–Al-acetate LDHs (0.77 mmol g^{-1}). Overall, MMOs derived from Mg–Al-acetate LDHs synthesized by modified acetamide hydrolysis showed better CO_2 capture and cycling stability than the MMOs derived from the anion exchanged and commercial LDHs.

4. Conclusions

In this work, we have successfully developed LDHs based novel MMOs with a mixed morphology and enhanced performance for high temperature (200–300 °C) CO_2 capture applications. The sorbents were synthesised by altering the starting precursors, synthesis method and hydrolysing agent. Mg–Al-acetate LDHs with two different Mg/Al ratios (3 and 4) were synthesized by employing metal hydroxides as precursors and acetamide as the hydrolysing agent. The acetamide acts both as a pH regulator and as the source of acetate ions. The resultant acetate intercalated LDHs crystallized in a new morphology having both fibrous and sheet-like particles. Interestingly, the derived MMOs retained the mixed morphology of the precursor LDHs. These MMOs showed high specific surface areas (316–341 m^2 g^{-1}) and enhanced CO_2 capture capacities under both 86 and 14% CO_2 atmospheres at ambient pressure. For instance, the CO_2 uptake at 200 °C (1.20 mmol g^{-1}) was almost double that of the value achieved by the MMOs derived from the anion exchanged acetate LDH (0.57 mmol g^{-1}) and the commercial LDH (0.67 mmol g^{-1}). The MMOs derived from Mg–Al-acetate LDHs synthesized by modified acetamide hydrolysis showed better CO_2 capture capacities compared to the MMOs derived from the anion exchanged and commercial LDHs. They also showed improved cyclic stability compared to the commercial LDH based MMOs. The starting precursors, synthesis method and hydrolysing agent used in this study have shown a positive effect on the CO_2 capture performance of the resultant MMOs.

Conflicts of interest

There are no conflicts to declare.

Acknowledgements

The authors gratefully acknowledge the financial support from the Engineering and Physical Sciences Research Council (EP/N024540/1) and the PrISMa Project (no 299659), which is funded through the ACT programme (Accelerating CCS Technologies, Horizon2020 Project No 294766). The authors also gratefully acknowledge the financial contributions from: BEIS together with extra funding from the NERC and the EPSRC, UK; RCN, Norway; SFOE, Switzerland and US-DOE, USA. The authors also gratefully acknowledge the additional financial support from TOTAL and Equinor.

References

1 P. M. Cox, R. A. Betts, C. D. Jones, S. A. Spall and I. J. Totterdell, *Nature*, 2000, **408**, 184–187.
2 P. Markewitz, W. Kuckshinrichs, W. Leitner, J. Linssen, P. Zapp, R. Bongartz, A. Schreiber and T. E. Müller, *Energy Environ. Sci.*, 2012, **5**, 7281–7305.
3 J. R. Fernández, S. Garcia and E. S. Sanz-Pérez, *Ind. Eng. Chem. Res.*, 2020, **59**, 6767–6772.
4 M. Pardakhti, T. Jafari, Z. Tobin, B. Dutta, E. Moharreri, N. S. Shemshaki, S. Suib and R. Srivastava, *ACS Appl. Mater. Interfaces*, 2019, **11**, 34533–34559.

5 T. N. Borhani and M. Wang, *Renewable Sustainable Energy Rev.*, 2019, 114.
6 G. T. Rochelle, in *Absorption-Based Post-combustion Capture of Carbon Dioxide*, Elsevier, 2016, pp. 35–67.
7 P. Moser, G. Wiechers, S. Schmidt, J. Garcia Moretz-Sohn Monteiro, C. Charalambous, S. Garcia and E. Sanchez Fernandez, *Int. J. Greenhouse Gas Control*, 2020, **95**, 102945.
8 B. Dutcher, M. Fan and A. G. Russell, *ACS Appl. Mater. Interfaces*, 2015, **7**, 2137–2148.
9 A. Samanta, A. Zhao, G. K. H. Shimizu, P. Sarkar and R. Gupta, *Ind. Eng. Chem. Res.*, 2012, **51**, 1438–1463.
10 K. Adil, P. M. Bhatt, Y. Belmabkhout, S. M. T. Abtab, H. Jiang, A. H. Assen, A. Mallick, A. Cadiau, J. Aqil and M. Eddaoudi, *Adv. Mater.*, 2017, **29**, 1702953.
11 L. K. G. Bhatta, S. Subramanyam, M. D. Chengala, S. Olivera and K. Venkatesh, *J. Cleaner Prod.*, 2015, **103**, 171–196.
12 Z. Yong, V. Mata and A. E. Rodrigues, *Ind. Eng. Chem. Res.*, 2001, **40**, 204–209.
13 E. L. G. Oliveira, C. A. Grande and A. E. Rodrigues, *Sep. Purif. Technol.*, 2008, **62**, 137–147.
14 Z. Yong and E. Rodrigues, *Energy Convers. Manage.*, 2002, **43**, 1865–1876.
15 M. Bellotto, B. Rebours, O. Clause, J. Lynch, D. Bazin and E. Elkaïm, *J. Phys. Chem.*, 1996, **100**, 8527–8534.
16 D. G. Evans and R. C. T. Slade, Layered double hydroxide, in *Structure & bonding*, ed. D. M. P. Mingos, Springer-Verlag, Berlin Heidelberg, 2006, vol. 119, pp. 1–87.
17 R. Ma and T. Sasaki, *Adv. Mater.*, 2010, **22**, 5082–5104.
18 V. R. Choudhary, P. A. Chaudhari and V. S. Narkhede, *Catal. Commun.*, 2003, **4**, 171–175.
19 Y. Gao, Z. Zhang, J. Wu, X. Yi, A. Zheng, A. Umar, D. O'Hare and Q. Wang, *J. Mater. Chem. A*, 2013, **1**, 12782–12790.
20 J. Wang, Y. Zhang, N. Altaf, D. O'Hare and Q. Wang, in *Inorganic Materials Series No. 1*, ed. Q. Wang, The Royal Society of Chemistry, 2018, pp. 1–60.
21 M. K. Ram Reddy, Z. P. Xu, G. Q. Lu and J. C. Diniz Da Costa, *Ind. Eng. Chem. Res.*, 2008, **47**, 2630–2635.
22 G. V. Manohara, M. M. Maroto-Valer and S. Garcia, *Dalton Trans.*, 2020, **49**, 923–931.
23 Q. Wang, Z. Wu, H. H. Tay, L. Chen, Y. Liu, J. Chang, Z. Zhong, J. Luo and A. Borgna, *Catal. Today*, 2011, **164**, 198–203.
24 C. T. Yavuz, B. D. Shinall, A. V. Iretskii, M. G. White, T. Golden, M. Atilhan, P. C. Ford and G. D. Stucky, *Chem. Mater.*, 2009, **21**, 3473–3475.
25 A. Garcia-Gallastegui, D. Iruretagoyena, V. Gouvea, M. Mokhtar, A. M. Asiri, S. N. Basahel, S. A. Al-Thabaiti, A. O. Alyoubi, D. Chadwick and M. S. P. Shaffer, *Chem. Mater.*, 2012, **24**, 4531–4539.
26 H. B. Mohd Sidek, Y. K. Jo, I. Y. Kim and S. J. Hwang, *J. Phys. Chem. C*, 2016, **120**, 23421–23429.
27 A. Garcia-Gallastegui, D. Iruretagoyena, M. Mokhtar, A. M. Asiri, S. N. Basahel, S. A. Al-Thabaiti, A. O. Alyoubi, D. Chadwick and M. S. P. Shaffer, *J. Mater. Chem.*, 2012, **22**, 13932–13940.
28 O. Aschenbrenner, P. McGuire, S. Alsamaq, J. Wang, S. Supasitmongkol, B. Al-Duri, P. Styring and J. Wood, *Chem. Eng. Res. Des.*, 2011, **89**, 1711–1721.
29 G. V. Manohara, *RSC Adv.*, 2014, **4**, 46126–46132.
30 X. Zhu, C. Chen, H. Suo, Q. Wang, Y. Shi, D. O'Hare and N. Cai, *Energy*, 2019, **167**, 960–969.
31 G. V. Manohara, L. Li, A. Whiting and H. C. Greenwell, *Dalton Trans.*, 2018, **47**, 2933–2938.
32 P. Sahoo, S. Ishihara, K. Yamada, K. Deguchi, S. Ohki, M. Tansho, T. Shimizu, N. Eisaku, R. Sasai, J. Labuta, D. Ishikawa, J. P. Hill, K. Ariga, B. P. Bastakoti, Y. Yamauchi and N. Iyi, *ACS Appl. Mater. Interfaces*, 2014, **6**, 18352–18359.
33 G. Hu and D. O'Hare, *J. Am. Chem. Soc.*, 2005, **127**, 17808–17813.
34 G. V. Manohara, D. A. Kunz, P. V. Kamath, W. Milius and J. Breu, *Langmuir*, 2010, **26**, 15586–15591.
35 G. V. Manohara and P. Vishnu Kamath, *Z. Anorg. Allg. Chem.*, 2014, **640**, 434–438.
36 J. W. Boclair and P. S. Braterman, *Chem. Mater.*, 1999, **11**, 298–302.
37 M. Rajamathi and P. Vishnu Kamath, *Bull. Mater. Sci.*, 2000, **23**, 355–359.
38 M. Ogawa and S. Asai, *Chem. Mater.*, 2000, **12**, 3253–3255.
39 H. C. Greenwell, W. Jones, S. L. Rugen-Hankey, P. J. Holliman and R. L. Thompson, *Green Chem.*, 2010, **12**, 688–695.
40 H. C. Greenwell, C. C. Marsden and W. Jones, *Green Chem.*, 2007, **9**, 1299–1307.
41 G. V. Manohara, P. Vishnu Kamath and W. Milius, *J. Solid State Chem.*, 2012, **196**, 356–361.
42 T. W. J. Taylor, *J. Chem. Soc.*, 1930, 2741–2750.
43 N. Iyi, Y. Ebina and T. Sasaki, *Langmuir*, 2008, **24**, 5591–5598.
44 U. Costantino, F. Marmottini, M. Nocchetti and R. Vivani, *Eur. J. Inorg. Chem.*, 1998, **1998**, 1439–1446.
45 H. R. Oswald and R. Asper, *Bivalent Metal Hydroxides*, 1977.
46 K. Nakamoto, *Infrared and Raman Spectra of Inorganic and Coordination Compounds: Part B: Applications in Coordination, Organometallic, and Bioinorganic Chemistry*, John Wiley and Sons, 2008.
47 M. Adachi-Pagano, C. Forano and J. P. Besse, *J. Mater. Chem.*, 2003, **13**, 1988–1993.
48 A. Yasukawa, T. Yokoyama and T. Ishikawa, *Mater. Res. Bull.*, 2001, **36**, 775–786.
49 H. Zhang and B. W. Darvell, *J. Am. Ceram. Soc.*, 2011, **94**, 2007–2013.
50 S. T. Zhang, Y. Dou, J. Zhou, M. Pu, H. Yan, M. Wei, D. G. Evans and X. Duan, *ChemPhysChem*, 2016, 2754–2766.
51 R. Warringham, S. Mitchell, R. Murty, R. Schäublin, P. Crivelli, J. Kenvin and J. Pérez-Ramírez, *Chem. Mater.*, 2017, **29**, 4052–4062.
52 L. A. Cheah, G. V. Manohara, M. M. Maroto-Valer and S. Garcia, *ChemistrySelect*, 2020, **5**, 5587–5594.
53 G. V. Manohara, A. Whiting and H. C. Greenwell, *ACS Omega*, 2019, **4**, 20230–20236.

54 M. Figlarz, B. Gérand, A. Delahaye-Vidal, B. Dumont, F. Harb, A. Coucou and F. Fievet, *Solid State Ionics*, 1990, **43**, 143–170.
55 F. Cavani, F. Trifirò and A. Vaccari, *Catal. Today*, 1991, **11**, 173–301.
56 M. Thommes, K. Kaneko, A. V. Neimark, J. P. Olivier, F. Rodriguez-Reinoso, J. Rouquerol and K. S. W. Sing, *Pure Appl. Chem.*, 2015, **87**, 1051–1069.
57 M. León, E. Díaz, S. Bennici, A. Vega, S. Ordóñez and A. Auroux, *Ind. Eng. Chem. Res.*, 2010, **49**, 3663–3671.
58 K. Coenen, F. Gallucci, B. Mezari, E. Hensen and M. van Sint Annaland, *J. CO_2 Util.*, 2018, **24**, 228–239.
59 Y. Zhang-zhu, W. Jing-jing, Z. Guang-ming, Z. Hua-zhang, T. Xiao-fei, C. Ma, L. Xue-cheng, L. Zi-hao and C. Zhang, *Coord. Chem. Rev.*, 2019, **386**, 154–182.
60 Q. Qin, J. Wang, T. Zhou, Q. Zheng, L. Huang, Y. Zhang, P. Lu, A. Umar, B. Louis and Q. Wang, *J. Energy Chem.*, 2017, **26**, 346–353.
61 L. K. G. Bhatta, S. Subramanyam, M. D. Chengala, S. Olivera and K. Venkatesh, *J. Cleaner Prod.*, 2015, **103**, 171–196.
62 X. Zhu, C. Chen, H. Suo, Q. Wang, Y. Shi, D. O'Hare and N. Cai, *Energy*, 2019, **167**, 960–969.
63 X. Kou, H. Guo, E. G. Ayele, S. Li, Y. Zhao, S. Wang and X. Ma, *Energy Fuels*, 2018, **32**, 5313–5320.
64 Q. Qin, J. Wang, T. Zhou, Q. Zheng, L. Huang, Y. Zhang, P. Lu, A. Umar, B. Louis and Q. Wang, *J. Energy Chem.*, 2017, **26**, 346–353.
65 S. Kim, S. G. Jeon and K. B. Lee, *ACS Appl. Mater. Interfaces*, 2016, **8**, 5763–5767.
66 Q. Wang, H. H. Tay, Z. Zhong, J. Luo and A. Borgna, *Energy Environ. Sci.*, 2012, **5**, 7526–7530.
67 S. Li, Y. Shi, Y. Yang, Y. Zheng and N. Cai, *Energy Fuels*, 2013, **27**, 5352–5358.
68 Y. Gao, Z. Zhang, J. Wu, X. Yi, A. Zheng, A. Umar, D. O'Hare and Q. Wang, *J. Mater. Chem. A*, 2013, **1**, 12782–12790.
69 N. D. Hutson and B. C. Attwood, *Adsorption*, 2008, **14**, 781–789.
70 S. J. Han, Y. Bang, H. J. Kwon, H. C. Lee, V. Hiremath, I. K. Song and J. G. Seo, *Chem. Eng. J.*, 2014, **242**, 357–363.